Highly Ca^{2+}-selective TRPM Channels Regulate IP_3-dependent Oscillatory Ca^{2+} Signaling in the *C. elegans* Intestine

Juan Xing, Xiaohui Yan, Ana Estevez, and Kevin Strange

Departments of Anesthesiology, Molecular Physiology and Biophysics, and Pharmacology, Vanderbilt University Medical Center, Nashville, TN 37232

Posterior body wall muscle contraction (pBoc) in the nematode *Caenorhabditis elegans* occurs rhythmically every 45–50 s and mediates defecation. pBoc is controlled by inositol-1,4,5-trisphosphate (IP_3)–dependent Ca^{2+} oscillations in the intestine. The intestinal epithelium can be studied by patch clamp electrophysiology, Ca^{2+} imaging, genome-wide reverse genetic analysis, forward genetics, and molecular biology and thus provides a powerful model to develop an integrated systems level understanding of a nonexcitable cell oscillatory Ca^{2+} signaling pathway. Intestinal cells express an outwardly rectifying Ca^{2+} (ORCa) current with biophysical properties resembling those of TRPM channels. Two TRPM homologues, GON-2 and GTL-1, are expressed in the intestine. Using deletion and severe loss-of-function alleles of the *gtl-1* and *gon-2* genes, we demonstrate here that GON-2 and GTL-1 are both required for maintaining rhythmic pBoc and intestinal Ca^{2+} oscillations. Loss of GTL-1 and GON-2 function inhibits I_{ORCa} ~70% and ~90%, respectively. I_{ORCa} is undetectable in *gon-2;gtl-1* double mutant cells. These results demonstrate that (a) both *gon-2* and *gtl-1* are required for ORCa channel function, and (b) GON-2 and GTL-1 can function independently as ion channels, but that their functions in mediating I_{ORCa} are interdependent. I_{ORCa}, I_{GON-2}, and I_{GTL-1} have nearly identical biophysical properties. Importantly, all three channels are at least 60-fold more permeable to Ca^{2+} than Na^+. Epistasis analysis suggests that GON-2 and GTL-1 function in the IP_3 signaling pathway to regulate intestinal Ca^{2+} oscillations. We postulate that GON-2 and GTL-1 form heteromeric ORCa channels that mediate selective Ca^{2+} influx and function to regulate IP_3 receptor activity and possibly to refill ER Ca^{2+} stores.

The Journal of General Physiology

Downloaded from http://rupress.org/jgp/article-pdf/131/3/245/1912627/jgp_200709914.pdf by guest on 05 December 2025

INTRODUCTION

The genetic model organism *Caenorhabditis elegans* provides numerous experimental advantages for developing an integrative genetic and molecular understanding of fundamental physiological processes (Barr, 2003; Strange, 2003). These advantages include a short life cycle, forward genetic tractability, a fully sequenced and well-annotated genome, and relative ease and economy of characterizing gene function using transgenic and RNA interference methods.

C. elegans intestinal epithelial cells generate rhythmic inositol 1,4,5-trisphosphate (IP_3)–dependent Ca^{2+} oscillations that control posterior body wall muscle contraction (pBoc) (Dal Santo et al., 1999; Espelt et al., 2005; Teramoto and Iwasaki, 2006; Peters et al., 2007). pBoc is part of a motor program that mediates defecation and can be observed readily through a dissecting microscope making it amenable to forward and reverse genetic screening (Thomas, 1990; Liu and Thomas, 1994; Iwasaki et al., 1995). Intestinal Ca^{2+} signaling can be quantified by imaging methods in isolated intestines (Espelt et al., 2005; Teramoto and Iwasaki, 2006; Peters et al., 2007) or in vivo using genetically encoded Ca^{2+} indicators (Teramoto and Iwasaki, 2006; Yan et al., 2006; Peters et al., 2007). Recent development of primary cell culture methods (Christensen et al., 2002; Strange et al., 2007) has made it possible to characterize intestinal ion channels using patch clamp methods (Estevez et al., 2003; Estevez and Strange, 2005; Yan et al., 2006; Lorin-Nebel et al., 2007). The ability to combine direct physiological measurements of IP_3–dependent oscillatory Ca^{2+} signals and associated ion channel activity with forward and reverse genetic screening is unique to *C. elegans*. The worm intestinal epithelium thus provides a powerful model system in which to define the genetic and molecular details and integrative physiology of oscillatory Ca^{2+} signaling in nonexcitable cells.

Intestinal Ca^{2+} oscillations are strictly dependent on Ca^{2+} release from the ER via ITR-1, the single IP_3 receptor encoded by the *C. elegans* genome (Dal Santo et al., 1999; Espelt et al., 2005; Teramoto and Iwasaki, 2006). Extensive studies in vertebrate (for reviews see Venkatachalam et al., 2002; Parekh and Putney, 2005; Hogan and Rao, 2007)

Correspondence to Kevin Strange: kevin.strange@vanderbilt.edu

A. Estevez's current address is Biology Department, St. Lawrence University, Canton, NY 13617.

Abbreviations used in this paper: CICR, Ca^{2+}-induced Ca^{2+} release; CRAC, Ca^{2+} release–activated Ca^{2+}; dsRNA, double-stranded RNA; IP_3, inositol-1,4,5-trisphosphate; ORCa, outwardly rectifying Ca^{2+}; pBoc, posterior body wall muscle contraction; SERCA, sarco/endoplasmic reticulum Ca^{2+} ATPase; SOCC, store-operated Ca^{2+} channel.

J. Gen. Physiol. © The Rockefeller University Press $30.00
Volume 131 Number 3 March 2008 245–255
http://www.jgp.org/cgi/doi/10.1085/jgp.200709914

and *Drosophila* cells (Yeromin et al., 2004) have demonstrated that depletion of ER Ca^{2+} stores activates store-operated Ca^{2+} channels (SOCCs). SOCCs are widely believed to be an essential and ubiquitous component of Ca^{2+} signaling pathways, functioning to refill ER Ca^{2+} stores and modulate intracellular Ca^{2+} signals (e.g., Venkatachalam et al., 2002; Parekh and Putney, 2005; Hogan and Rao, 2007). The most extensively studied and characterized SOCC is the Ca^{2+} release–activated Ca^{2+} (CRAC) channel (Parekh and Putney, 2005). The CRAC channel pore is comprised of Orai1/CRACM and channel activation is mediated by STIM1, which functions as an ER Ca^{2+} sensor (for reviews see Hogan and Rao, 2007; Lewis, 2007; Putney, 2007).

C. elegans intestinal cells express robust CRAC channel activity (Estevez et al., 2003). RNAi silencing of *orai-1* or *stim-1*, which encode worm Orai1/CRACM and STIM1 homologues, dramatically reduces CRAC channel expression and function, but surprisingly has no effect on intestinal Ca^{2+} signaling (Lorin-Nebel et al., 2007; Yan et al., 2006). These findings suggest that CRAC channels are not essential components of IP_3-dependent Ca^{2+} signaling in the intestine and indicate that other Ca^{2+} entry mechanisms must function to maintain intestinal Ca^{2+} oscillations.

In addition to CRAC channels, intestinal cells express a store-independent outwardly rectifying Ca^{2+} (ORCa) channel that has biophysical properties resembling those of mammalian TRPM channels (Estevez et al., 2003). Three TRPM homologues are encoded by the *C. elegans* genome, GON-2, GTL-1, and GTL-2 (Kahn-Kirby and Bargmann, 2006; Baylis and Goyal, 2007). GFP reporter studies have demonstrated that intestinal cells express *gon-2* and *gtl-1* (Teramoto et al., 2005; cited as unpublished observations in Baylis and Goyal, 2007; WormBase, http://www.wormbase.org/). The goal of the present study was to define the roles these genes play in intestinal Ca^{2+} signaling. Our results demonstrate that GON-2 and GTL-1 are both required for ORCa channel activity and for maintaining rhythmic Ca^{2+} oscillations. We propose that *gon-2* and *gtl-1* encode the ORCa channel. We also suggest that ORCa channels comprise a major Ca^{2+} entry pathway in intestinal epithelial cells and that they function to regulate IP_3 receptor activity and refill ER Ca^{2+} stores.

MATERIAL AND METHODS

C. elegans Strains

Nematodes were cultured using standard methods on nematode growth medium (NGM) (Brenner, 1974). Wild-type worms were the Bristol N2 strain or *elt-2::gfp* worms that express a transcriptional GFP reporter in intestinal cell nuclei. Worms homozygous for the *gon-2* loss-of-function allele *gon-2(q388)* or the *gtl-1* deletion allele *gtl-1(ok375)* were used for studies of GON-2 and GTL-1 function. *gon-2;gtl-1* double mutant worms were generated by crossing the *gtl-1(ok375)* and *gon-2(q388)* strains (Teramoto et al., 2005). The *gon-2;gtl-1* double mutant worm strain exhibits greatly slowed larval development on NGM. To improve development and fertility sufficiently for experiments to be performed, double mutants were grown on NGM supplemented with 20 mM Mg^{2+} (see Teramoto et al., 2005). All worm strains were maintained at 16–20°C. Growth temperatures used in specific experiments are described below.

Characterization of pBoc Cycle

gon-2(q388) is a temperature sensitive allele and the mutant phenotype is observed at growth temperatures of 25°C (Sun and Lambie, 1997). For posterior body wall muscle contraction (pBoc) measurements, eggs from wild-type and mutant worm strains were cultured in a 25°C incubator until adulthood. The times required for wild-type, *gon-2* mutant, *gtl-1* mutant, and double mutant worms to reach adulthood at 25°C were 2–3 d, 3–4 d, 3–4 d, and 5 d, respectively.

pBoc was monitored by imaging worms on growth agar plates using a Carl Zeiss MicroImaging Inc. Stemi SV11 M^2BIO stereo dissecting microscope (Kramer Scientific Corp.) equipped with a DAGE-MTI DC2000 CCD camera. A minimum of 10 pBoc cycles were measured in each animal. Measurements were performed at a room air temperature of 22–23°C. Agar temperature was monitored during the course of pBoc measurements using a thermistor (Model 4600, Yellow Springs Instruments) and was 24–25°C.

Dissection and Fluorescence Imaging of Intestines

Worms were cultured as described above for pBoc measurements. Calcium oscillations were measured in isolated intestines as described previously (Espelt et al., 2005). In brief, worms were placed in control saline (137 mM NaCl, 5 mM KCl, 1 mM $MgCl_2$, 1 mM $MgSO_4$, 0.5 mM $CaCl_2$, 10 mM HEPES, 5 mM glucose, 2 mM L-asparagine, 0.5 mM L-cysteine, 2 mM L-glutamine, 0.5 mM L-methionine, 1.6 mM L-tyrosine, 28 mM sucrose, pH 7.3, 340 mOsm) and cut behind the pharynx using a 26-gauge needle. The hydrostatic pressure in the worm spontaneously extruded the intestine, which remained attached to the rectum and the posterior end of the animal. Isolated intestines were incubated for 15 min in bath saline containing 5 μM fluo-4 AM and 1% BSA. Imaging was performed using a Nikon TE2000 inverted microscope, a Superfluor 40X/1.3 N.A. oil objective lens, a Photometrics Cascade 512B cooled CCD camera (Roper Industries), and MetaFluor software (Molecular Devices Corporation). Room temperature was maintained at 25–26°C. Fluo-4 was excited using a 490-500BP filter and a 523-547BP filter was used to detect fluorescence emission. Fluorescence images were acquired at 0.2 or 1 Hz. Changes in fluo-4 intensity were quantified in posterior-to-anterior moving Ca^{2+} waves using region-of-interest selection and MetaFluor software (Molecular Devices Corporation).

C. elegans Embryonic Cell Culture and Patch Clamp Electrophysiology

Newly hatched wild type and mutant worm L1 larvae were cultured at 25°C until adulthood. Embryonic cells were cultured for 2–3 d at 25°C on 12-mm diameter acid-washed glass coverslips using established methods (Christensen et al., 2002; Strange et al., 2007). To maximize suppression of GON-2 activity, cells isolated from *gon-2* and *gon-2;gtl-1* double mutant worms were cultured in the presence of *gon-2* double stranded RNA (dsRNA) using methods described previously (Yan et al., 2006; Lorin-Nebel et al., 2007). *gon-2* dsRNA was synthesized from a 640-bp (4041–4681-bp) *gon-2* cDNA that was amplified from a *C. elegans* cDNA library.

Coverslips with cultured embryo cells were placed in the bottom of a bath chamber (model R-26G; Warner Instrument Corp.) that was mounted onto the stage of a Nikon TE2000 inverted microscope. Bath temperature was maintained at 25°C using a Warner Instruments model SC-20 dual in-line heater/cooler, a model CL-100 bipolar temperature controller, and a PHC series heater/cooler jacket for the bath chamber. Cells were visualized by fluorescence and video-enhanced DIC microscopy. Intestinal cells were identified

Downloaded from http://rupress.org/jgp/article-pdf/131/3/245/1912627/jgp_200709914.pdf by guest on 05 December 2025

in culture by expression of the intestine-specific reporter *elt-2*::GFP or by morphological characteristics (Fukushige et al., 1998; Estevez et al., 2003).

Patch electrodes were pulled from soft glass capillary tubes (PG10165-4, World Precision Instruments) that had been silanized with dimethyl-dichloro silane. Pipette resistance was 4–7 MΩ. Bath and pipette solutions contained 145 mM NaCl, 1 mM $CaCl_2$, 5 mM $MgCl_2$, 10 mM HEPES, 20 mM glucose, pH 7.2 (adjusted with NaOH), and 147 mM sodium gluconate (NaGluconate), 0.6 mM $CaCl_2$, 1 mM $MgCl_2$, 10 mM EGTA, 10 mM HEPES, 2 mM Na_2ATP, 0.5 mM Na_2GTP, pH 7.2 (adjusted with CsOH), respectively. The osmolality of bath and pipette solutions were adjusted to 345–350 mOsm and 325–330 mOsm using sucrose.

Whole cell currents were recorded using an Axopatch 200B (Axon Instruments) patch clamp amplifier. Command voltage generation, data digitization, and data analysis were performed on a 2.79 GHz Pentium computer (Dimension 9150; Dell Computer Corp.) using a Digidata 1322A AD/DA interface with pClamp 10 software (Axon Instruments). Electrical connections to the amplifier were made using Ag/AgCl wires and 3 M KCl/agar bridges.

Currents were elicited using a ramp or step voltage clamp protocol. For the ramp protocol, membrane potential was held at 0 mV and ramped from −80 to +80 mV at 215 mV/s every 5 s. Step changes in whole cell current were elicited by stepping membrane voltage from −80 to +80 mV in 20-mV steps from a holding potential of 0 mV. Voltage steps were maintained for 400 ms. Cell capacitances for all cells studied ranged from 1 to 4 pF.

As we described previously, I_{ORCa} is outwardly rectifying with a strongly positive reversal potential (Estevez et al., 2003). In the present study, we also observed that currents in *gon-2* and *gtl-1* mutant cells reversed at strongly positive membrane potentials and exhibited outward rectification. Outwardly rectifying currents with reversal potentials <10 mV were deemed to be excessively contaminated with nonspecific leak current and were rejected from final datasets.

Ion substitution studies were performed by replacement of bath Na^+ with various test cations. Cells were patch clamped initially in control bath solution until whole cell current had stabilized and then switched to a Ca^{2+}- and Mg^{2+}-free medium containing 1 mM EGTA. Changes in reversal potential (E_{rev}) were measured after replacement of 150 mM bath NaCl with 150 mM NMDG-Cl, 130 mM NMDG-Cl, and 10 mM $CaCl_2$ or 130 mM NMDG-Cl and 10 mM $MgCl_2$. Liquid junction potential changes were calculated using pClamp 10. Reversal potentials during ion substitution experiments were corrected for liquid junction potentials. Relative permeabilities were calculated from E_{rev} changes as described previously (Estevez et al., 2003).

Induction of RNA Interference by Double Strand RNA Feeding

RNA interference was induced by feeding *gon-2;gtl-1* double mutant worms bacteria producing dsRNA (e.g., Kamath et al., 2000; Rual et al., 2004) homologous to PLCγ or PLCβ. RNAi bacterial strains were engineered as described previously (Yin et al., 2004). Bacterial strains were streaked to single colonies on agar plates containing 50 μg/ml ampicillin and 12.5 μg/ml tetracycline. Single colonies were used to inoculate LB media containing 50 μg/ml ampicillin and cultures were grown at 37°C for 16–18 h with shaking. 300 μl of each bacterial culture were seeded onto 60-mm NGM agar plates containing 20 mM Mg^{2+}, 50 μg/ml ampicillin, and 1 mM IPTG to induce dsRNA synthesis. After seeding, plates were left at room temperature overnight. Eggs were transferred to the RNAi feeding plates and grown at 25°C.

Statistical Analysis

Data are presented as means ± SEM. Statistical significance was determined using Student's two-tailed *t* test for unpaired means. When comparing three or more groups, statistical significance was determined by one-way analysis of variance with a Bonferroni post-hoc test. P values of ≤0.05 were taken to indicate statistical significance. The rhythmicity of the pBoc cycle and intestinal Ca^{2+} oscillations is quantified as coefficient of variance, which is the standard deviation expressed as a percentage of the sample mean.

RESULTS

Removal of Extracellular Ca^{2+} Causes Rapid Cessation of Intestinal Ca^{2+} Oscillations

Calcium is taken up into the ER via the sarco/endoplasmic reticulum Ca^{2+} ATPase (SERCA) while plasma membrane pumps and exchangers continuously extrude Ca^{2+} from the cell (Berridge et al., 2003; Hogan and Rao, 2007). Because of the presence of plasma membrane Ca^{2+} extrusion mechanisms, some Ca^{2+} will be lost from the cell during ER Ca^{2+} release. Repeated and/or prolonged ER Ca^{2+} release will eventually deplete ER Ca^{2+} stores and prevent further IP_3-dependent Ca^{2+} signals unless plasma membrane Ca^{2+} entry mechanisms are also active. To determine whether such Ca^{2+} entry mechanisms are required for IP_3-dependent Ca^{2+} signaling in the intestine, we monitored Ca^{2+} oscillations during removal of bath Ca^{2+}. As shown in Fig. 1, total intracellular fluo-4 fluorescence dropped and Ca^{2+} oscillations ceased rapidly when extracellular Ca^{2+} was removed. Calcium oscillations recovered when Ca^{2+} was added back to the bath. These results demonstrate that Ca^{2+} entry mechanisms are active in the intestine and that Ca^{2+} oscillations are strictly dependent on extracellular Ca^{2+} influx. Calcium entry almost certainly functions to refill ER stores. In addition, Ca^{2+} influx may modulate IP_3 receptor activity and/or contribute to the total increase in cytoplasmic Ca^{2+} concentration during Ca^{2+} oscillations.

The TRPM Channels GTL-1 and GON-2 Are Required for Normal Intestinal Ca^{2+} Signaling

As discussed in the Introduction, loss of function of CRAC channels and the ER Ca^{2+} sensor STIM-1 has no effect on oscillatory Ca^{2+} signaling in the *C. elegans* intestine (Lorin-Nebel et al., 2007; Yan et al., 2006). Other channels must therefore mediate Ca^{2+} entry. Given that *gon-2* and *gtl-1* are expressed in the intestine (Teramoto et al., 2005; cited as unpublished observations in Baylis and Goyal, 2007; WormBase, http://www.wormbase.org/), we quantified pBoc and intestinal Ca^{2+} oscillations in animals harboring loss-of-function mutations in these genes. *gtl-1(ok375)* is a 2,714-bp deletion allele that deletes all of the predicted transmembrane domains of GTL-1 and is almost certainly null. *gon-2(q388)* is a point mutation in which glutamate 955 is mutated to lysine (West et al., 2001). Glutamate 955 is highly conserved in human, mouse, *Drosophila*, and *C. elegans* TRP channels and mutation to lysine most likely causes temperature-sensitive disruption of a step in GON-2 synthesis (West et al., 2001). The E955K mutation induces a severe

Downloaded from http://rupress.org/jgp/article-pdf/131/3/245/1912627/jgp_200709914.pdf by guest on 05 December 2025

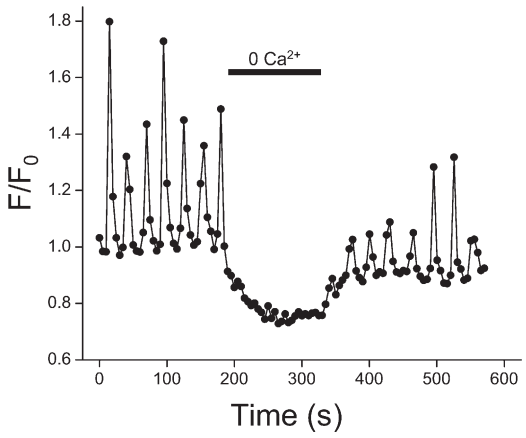

Figure 1. Requirement of intestinal Ca^{2+} oscillations on extracellular Ca^{2+}. Representative experiment showing the effect of extracellular Ca^{2+} removal on Ca^{2+} oscillations. Calcium-free extracellular solution was buffered with 1 mM EGTA. Removal of bath Ca^{2+} causes rapid inhibition of Ca^{2+} oscillations and drop in total fluo-4 fluorescence (similar results were observed in five out five intestines). Addition of Ca^{2+} back to the bath causes a rapid increase in fluo-4 fluorescence and recovery of Ca^{2+} oscillations (similar results were observed in four out of four intestines).

loss-of-function phenotype when worms are grown at 25°C (Sun and Lambie, 1997; Church and Lambie, 2003). As noted earlier, the *gon-2;gtl-1* double mutant was derived from a cross of *gtl-1(ok375)* and *gon-2(q388)* worms (Teramoto et al., 2005).

Fig. 2 A shows pBoc cycles in individual wild-type and channel mutant worms. Coefficients of variance were calculated as a measure of cycle rhythmicity. Wild-type worms exhibited a highly rhythmic pBoc cycle with coefficients of variance for individual animals ranging from 2 to 5%. In striking contrast, loss of activity of either channel disrupted pBoc rhythmicity. Coefficients of variance ranged from 3 to 33% and 7 to 28% for GTL-1 and GON-2 mutant worms, respectively. Disruption of pBoc was more severe in the double mutant worms where coefficients of variance ranged from 10 to 67%.

pBoc cycle data are summarized in Fig. 2 B. Mean cycle periods and coefficients of variance were increased significantly ($P < 0.05$) in *gtl-1* mutant, *gon-2* mutant, and double mutant worms. In addition, the mean coefficient of variance was significantly ($P < 0.01$) greater in the double mutant worms compared with either GTL-1 or GON-2 mutant animals.

As discussed in the Materials and methods section, double mutant worms develop and reproduce poorly unless the Mg^{2+} concentration in the growth agar is increased to 20 mM. To determine whether high Mg^{2+} has any effect on the pBoc cycle, we grew wild-type worms for one generation on high Mg^{2+} plates. Mean ± SEM pBoc period and coefficient of variance were 43 ± 1 s and 3.5 ± 0.7% ($n = 6$), respectively, and were not significantly ($P > 0.3$) different from those of worms grown on standard NGM agar (see Fig. 2 B).

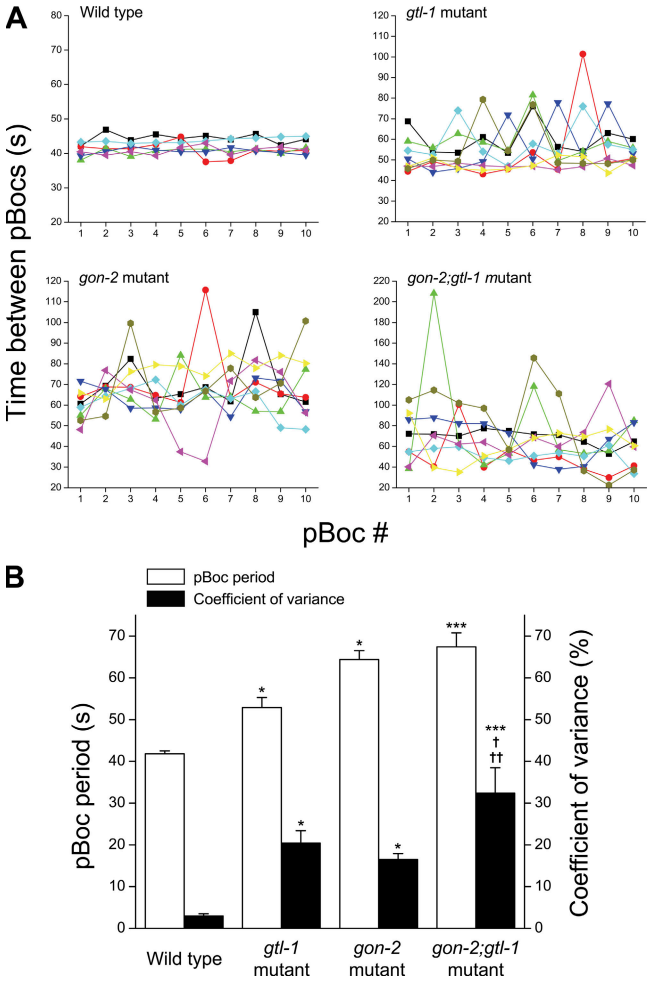

Figure 2. Effect of *gtl-1* and *gon-2* loss-of-function mutations on pBoc period and rhythmicity. (A) pBoc cycles in individual wild-type, GTL-1 mutant, GON-2 mutant, and double mutant worms. Different colors and symbols represent different animals. (B) pBoc periods and rhythmicity for wild type and GTL-1 and GON-2 mutant worm strains. Cycle rhythmicity is quantified as coefficient of variance. Values are means ± SEM ($n = 6$–23). *, $P < 0.05$; ***, $P < 0.001$, compared with wild type worms. †, $P < 0.01$, compared with GTL-1 mutant worms. ††, $P < 0.001$, compared with GON-2 mutant worms. All worm strains were grown at 25°C.

Intestinal IP_3-dependent Ca^{2+} oscillations drive pBoc through a yet to be defined mechanism (Dal Santo et al., 1999; Espelt et al., 2005; Teramoto and Iwasaki, 2006; Peters et al., 2007). To determine whether GTL-1 and GON-2 function in Ca^{2+} signaling, we quantified Ca^{2+} oscillations in intestines dissected from wild-type and mutant animals. Calcium oscillations were arrhythmic in intestines isolated from GTL-1, GON-2, and double mutant worms (Fig. 3 A). Mean coefficients of variance were increased significantly ($P < 0.05$) by 2.3–3.2-fold in the single and double mutants (Fig. 3 B). Due to intracycle and animal-to-animal variability, the mean oscillation periods were not significantly ($P > 0.05$) different for the three groups of mutant worms and wild-type animals (unpublished data). Oscillation kinetics as measured by

Downloaded from http://rupress.org/jgp/article-pdf/131/3/245/1912627/jgp_200709914.pdf by guest on 05 December 2025

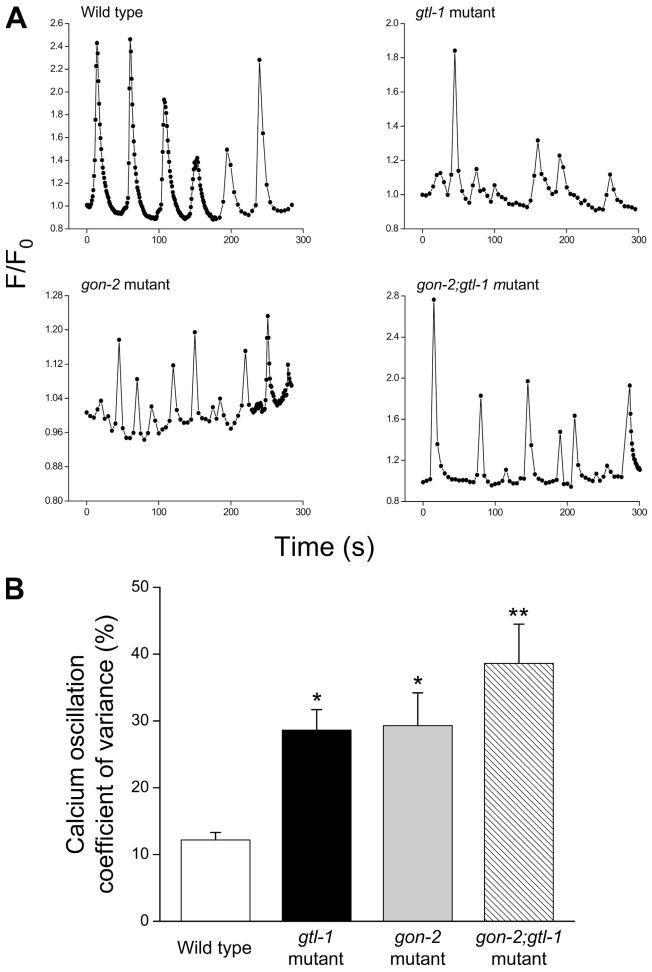

Figure 3. Effect of *gtl-1* and *gon-2* loss-of-function mutations on intestinal Ca^{2+} oscillation rhythmicity. (A) Calcium oscillations in single intestines isolated from wild-type, GTL-1 mutant, GON-2 mutant, and double mutant worms. (B) Calcium oscillation rhythmicity in wild-type and mutant worm intestines. Rhythmicity is quantified as coefficient of variance. Values are means ± SEM (n = 6–10). *, $P < 0.05$; **, $P < 0.001$, compared with wild-type worms. All worm strains were grown at 25°C.

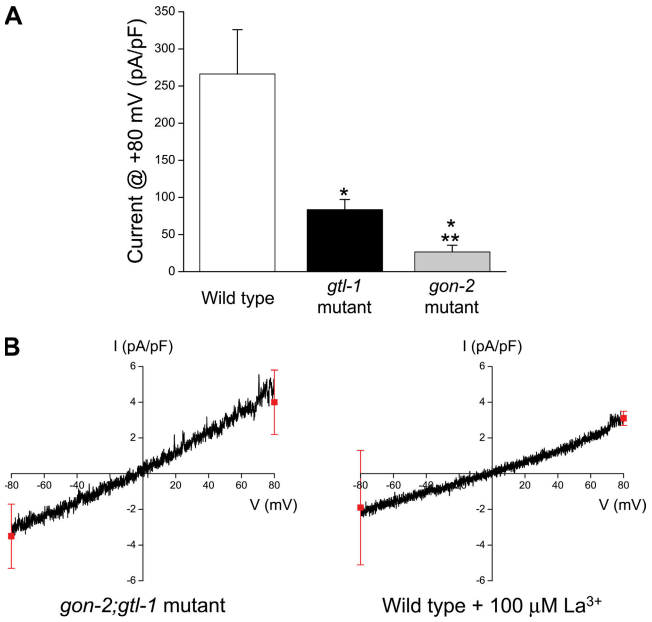

Figure 4. Effect of *gtl-1* and *gon-2* loss-of-function mutations on whole cell current. (A) Mean whole cell current amplitude in intestinal cells cultured from wild-type, *gtl-1* mutant, and *gon-2* mutant worms. Values are means ± SEM (n = 11–22). *, $P < 0.01$, compared with wild-type worms. **, $P < 0.002$, compared with *gtl-1* mutant worms. All worm strains were grown at 25°C. (B) Current-to-voltage relationships of whole cell currents measured in intestinal cells cultured from wild-type and *gon-2;gtl-1* double mutant worms. Wild-type intestinal cells were patch clamped in a bath solution containing 100 mM La^{3+}, which completely inhibits I_{ORCa} (see Fig. 6 A). Remaining current shows a near linear current-to-voltage relationship and E_{rev} near 0 mV and is defined as leak current. Current-to-voltage relationship of *gon-2;gtl-1* double mutant whole cell currents is also near linear with a near 0 E_{rev}. Data shown are the means of currents recorded from four wild-type cells and five *gon-2;gtl-1* double mutant cells. Currents were elicited by ramping membrane potential from −80 to + 80 mV at 215 mV/s. Red symbols and error bars are mean ± SEM error currents measured at holding potentials of −80 and + 80 mV. Mean currents measured at −80 and + 80 mV and E_{rev} values were not significantly ($P > 0.3$) different for wild-type cells treated with La^{3+} and *gon-2;gtl-1* double mutant cells.

oscillation rise and fall times were unaffected ($P > 0.05$) by channel mutations (unpublished data). We conclude from data shown in Figs. 2 and 3 that GTL-1 and GON-2 are both required for maintaining the rhythmicity of Ca^{2+} oscillations in the *C. elegans* intestinal epithelium.

GTL-1 and GON-2 Mediate Whole Cell Outwardly Rectifying Ca^{2+} Currents

We suggested previously that I_{ORCa} may play an important role in generating intestinal Ca^{2+} oscillations (Estevez et al., 2003; Estevez and Strange, 2005). To determine whether the ORCa channel is encoded by *gon-2* and/or *gtl-1*, we characterized whole cell cation currents in intestinal cells cultured from wild-type, *gon-2* mutant, *gtl-1* mutant, and *gon-2;gtl-1* double mutant worms. I_{ORCa} in wild-type intestinal cells is constitutively active and undergoes additional slow activation for 1–2 min after whole cell recording is initiated (Estevez et al., 2003). Mean ORCa current density at +80 mV measured 4–5 min after membrane rupture in wild-type cells was 266 pA/pF (Fig. 4 A). The mean ± SEM reversal potential (E_{rev}) of I_{ORCa} was 18 ± 1 mV (n = 22). The positive reversal potential is expected for a Ca^{2+}-selective channel (Estevez et al., 2003).

Whole cell current density was strikingly and significantly ($P < 0.01$) suppressed in intestinal cells cultured from both *gon-2* and *gtl-1* mutant worms. In both groups of cells, the majority of currents we observed were outwardly rectifying with a strongly positive E_{rev} similar to that of I_{ORCa}. In 2 out 11 *gon-2* mutant cells, whole cell current exhibited an E_{rev} close to zero and a near-linear current-to-voltage relationship. We interpreted these observations as indicating that loss of function of *gon-2* in these cells completely suppressed I_{ORCa} and that whole

Downloaded from http://rupress.org/jgp/article-pdf/131/3/245/1912627/jgp_200709914.pdf by guest on 05 December 2025

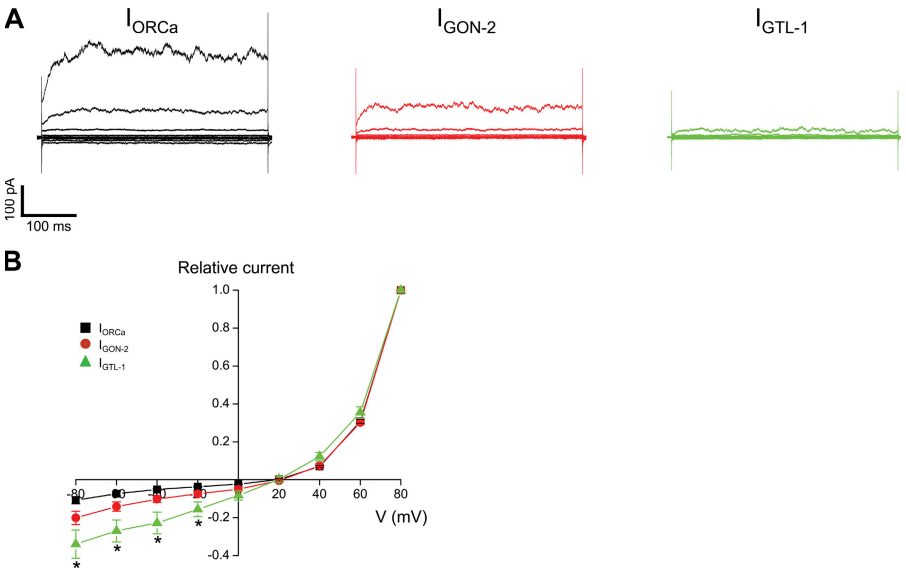

Figure 5. Current-to-voltage characteristics of I_{ORCa}, I_{GTL-1}, and I_{GON-2}. (A) Representative whole cell currents recorded from wild-type, *gtl-1* mutant, and *gon-2* mutant worm intestinal cells. Currents were elicited by stepping membrane voltage from −80 to +80 mV in 20-mV steps from a holding potential of 0 mV. (B) Relative current-to-voltage relationships of I_{ORCa}, I_{GTL-1}, and I_{GON-2}. Values are means ± SEM (n = 9–22). *, $P < 0.001$, compared with I_{ORCa}. I_{GTL-1} and I_{GON-2} are currents measured in intestinal cells isolated from *gon-2* and *gtl-1* mutant worms, respectively.

cell conductance was due largely to a nonselective leak current. Mean current density was 26.5 pA/pF in *gon-2* cells and 83.5 pA/pF in *gtl-1* cells (Fig. 4 A). Currents recorded from all *gtl-1* cells showed outward rectification and had a mean ± SEM E_{rev} of 19 ± 1 mV (n = 21). The mean ± SEM E_{rev} value for the outwardly rectifying currents observed in *gon-2* mutant cells was 18 ± 2 mV (n = 9). Mean reversal potentials of outwardly rectifying currents in *gon-2* and *gtl-1* mutant cells were not significantly ($P < 0.05$) different from that observed in wild-type cells.

In five out of five *gon-2;gtl-1* double mutant cells, a small current with a near-linear current-to-voltage relationship was detected. The mean ± SEM E_{rev} for this current was 1.1 ± 2.7 mV (n = 5), which is not significantly ($P > 0.7$) different from 0 (Fig. 4 B). To determine whole cell current properties in the absence of I_{ORCa}, we patch clamped wild-type intestinal cells and bathed them with 100 μM La^{3+}, which completely inhibits ORCa channel activity (see Fig. 6 A). A small near-linear current with an E_{rev} (mean ± SEM = −1.6 ± 1.5 mV; n = 5) not significantly ($P > 0.3$) different from 0 was recorded in these cells (Fig. 4 B). We define this current as nonselective leak current. Mean ± SEM whole cell currents measured at −80 mV and +80 mV in *gon-2;gtl-1* double mutant cells and wild-type cells treated with 100 μM La^{3+} were −3.5 ± 1.8 pA/pF and 4.0 ± 1.8 pA/pF (n = 5) and −1.9 ± 3.2 pA/pF and 3.1 ± 0.4 pA/pF (n = 5), respectively, and were not significantly ($P > 0.6$) different (Fig. 4 B). Treatment of *gon-2;gtl-1* mutant cells with 100 μM La^{3+} had no significant ($P > 0.2$) on whole cell current amplitude (mean ± SEM whole cell currents measured at −80 and +80 mV were −4.9 ± 1.0 and 8.3 ± 3.8 pA/pF, respectively; n = 3). These results demonstrate that combined loss of GON-2 and GTL-1 activity completely suppresses I_{ORCa}. We therefore conclude that I_{ORCa} is mediated by the function of both channels.

Functional Properties of GON-2 and GTL-1 Mediated Whole Cell Currents

The inhibitory effects of loss of GON-2 or GTL-1 alone on I_{ORCa} are not additive; whole cell current density was reduced ∼90% and ∼70% in *gon-2* and *gtl-1* mutant cells, respectively (Fig. 4 A). These results indicate that (a) GON-2 and GTL-1 can function independently as ion channels, but (b) their functions in mediating I_{ORCa} are somehow interdependent (see Discussion). We define the currents observed in *gon-2* and *gtl-1* mutant cells as I_{GTL-1} and I_{GON-2}, respectively.

To further define the roles of GON-2 and GTL-1 in mediating I_{ORCa}, we characterized the biophysical properties of I_{GTL-1} and I_{GON-2}. Fig. 5 shows representative ORCa (i.e., wild type), GON-2, and GTL-1 currents and relative current-to-voltage relationships. All three currents show similar outward rectification. However, relative inward GTL-1 currents at −20 to −80 mV were slightly but significantly ($P < 0.001$) greater than that of I_{ORCa} (Fig. 5 B).

I_{ORCa} was inhibited by extracellular La^{3+} with a mean ± SEM IC_{50} of 3.7 ± 0.6 μM (n = 6). The La^{3+} dose–response relationships for I_{GON-2} and I_{GTL-1} were superimposable with that of I_{ORCa} (Fig. 6 A). Mean ± SEM La^{3+} IC_{50} values were 5.7 ± 1.8 μM (n = 6) and 5.3 ± 1.5 μM (n = 4) for I_{GON-2} and I_{GTL-1}, respectively, and were not significantly ($P > 0.05$) different from that of I_{ORCa}.

Fig. 6 B shows cation permeabilities measured under bi-ionic conditions of the ORCa, GON-2, and GTL-1 channels relative to Na^+ (i.e, P_{cation}/P_{Na}). The P_{NMDG}/P_{Na}, P_{Ca}/P_{Na}, and P_{Mg}/P_{Na} for the channels were not significantly ($P > 0.05$) different and ranged between 0.07 and 0.1, 57 and 66, and 3 and 6, respectively.

Increasing intracellular Mg^{2+} concentration inhibits I_{ORCa} (Fig. 6 C) (Estevez et al., 2003). The Mg^{2+} dose–response relationships for I_{ORCa}, I_{GON-2}, and I_{GTL-1} were similar (Fig. 6 C). IC_{50} values derived from fits to mean values in the datasets were 420 μM for I_{ORCa}, 440 μM for

Downloaded from http://rupress.org/jgp/article-pdf/131/3/245/1912627/jgp_200709914.pdf by guest on 05 December 2025

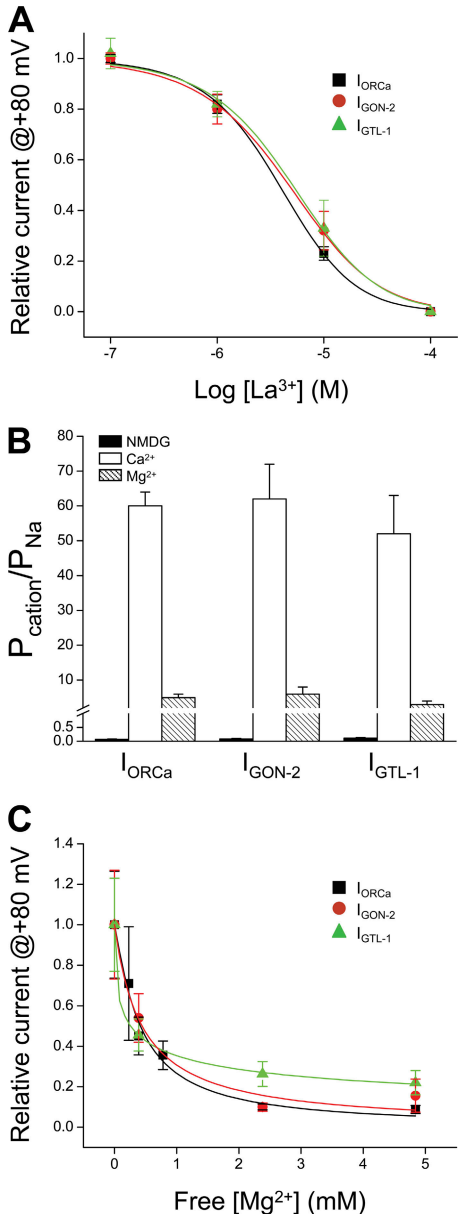

Figure 6. Lanthanum and Mg^{2+} sensitivity and relative cation permeabilities of the ORCa, GTL-1, and GON-2 channels. (A) Dose–response relationship for the inhibitory effect of extracellular La^{3+} on I_{ORCa}, I_{GTL-1}, and I_{GON-2}. Data were fit using the equation $I = 1/1 + ([La^{3+}]/IC_{50})^n$. Values are means ± SEM (n = 4–6). (B) Relative cation permeabilities of the ORCa, GTL-1, and GON-2 channels. Values are means ± SEM (n = 4–9). (C) Dose–response relationship for the inhibitory effect of intracellular Mg^{2+} on I_{ORCa}, I_{GTL-1}, and I_{GON-2}. Data were fit using the equation $I = 1/1 + ([Mg^{2+}]/IC_{50})^n$. Values are means ± SEM (n = 4–8). I_{GTL-1} and I_{GON-2} are currents measured in intestinal cells isolated from *gon-2* and *gtl-1* mutant worms, respectively.

I_{GON-2}, and 260 μM for I_{GTL-1}. Comparison of the fits indicated that the three datasets were not significantly ($P > 0.05$) different from one another.

It has been suggested that GON-2 and GTL-1 play a central role in intestinal Mg^{2+} uptake (Teramoto et al., 2005). The ORCa, GON-2, and GTL-1 channels clearly

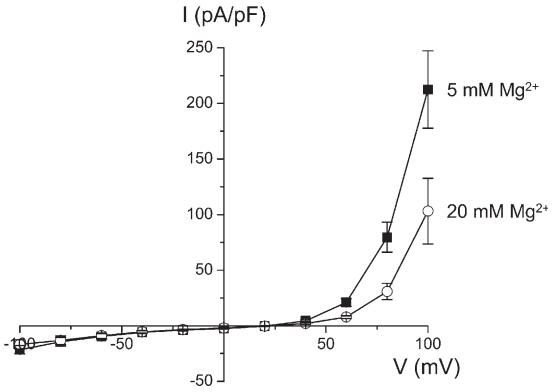

Figure 7. Effect of increasing bath Mg^{2+} concentration on whole cell current amplitude and E_{rev} in the presence of 1 mM Ca^{2+}. No significant ($P > 0.3$) shift in E_{rev} or inward current was detected when Mg^{2+} concentration was raised fourfold to 20 mM. Values are means ± SEM (n = 4).

have measurable Mg^{2+} permeabilities under bi-ionic conditions. However, given that the relative Ca^{2+} permeabilities of the channels are at least an order of magnitude greater than that of Mg^{2+} (Fig. 6 B and Teramoto et al., 2005), a more physiologically relevant question is whether significant Mg^{2+} permeation occurs when Ca^{2+} is present in the extracellular medium. To address this question, we patch clamped wild-type intestinal cells in a modified standard bath solution containing 130 mM NaCl and 30 mM NMDG-Cl and the normal Ca^{2+} and Mg^{2+} concentrations of 1 mM and 5 mM, respectively. When current amplitude had stabilized, the NMDG-Cl was replaced with 15 mM $MgCl_2$. In the presence of 1 mM bath Ca^{2+}, the mean ± SEM shifts in E_{rev} and current density at −80 mV observed when bath Mg^{2+} levels were raised fourfold were 0.7 ± 0.5 mV (n = 4) and −1.6 ± 1.7 pA/pF (n = 4), respectively (Fig. 7). These values were not significantly ($P > 0.3$) different from zero suggesting that Mg^{2+} permeation through the ORCa channel is very low in the presence of Ca^{2+}. Studies designed to directly quantify net Mg^{2+} influx through the ORCa channel under physiologically relevant conditions are needed to fully define its role in intestinal Mg^{2+} uptake and whole animal Mg^{2+} homeostasis.

Physiological Roles of GON-2 and GTL-1

As shown in Figs. 2 and 3, loss of *gon-2* and/or *gtl-1* activity dramatically disrupts pBoc rhythmicity and intestinal Ca^{2+} signaling. Teramoto et al. (2005) observed that the pBoc cycle was prolonged and apparently arrhythmic in *gon-2;gtl-1* double mutant worms and that the defect was fully rescued by increasing the Mg^{2+} concentration of the growth agar to 40 mM. They suggested that the altered defecation cycle was due to an alteration in the physiological state of the intestine resulting from Mg^{2+} deficiency. In our hands, the pBoc defect in double mutant worms was unaffected by external Mg^{2+} levels of either 20 (Fig. 2) or 40 mM (unpublished data).

Downloaded from http://rupress.org/jgp/article-pdf/131/3/245/1912627/jgp_200709914.pdf by guest on 05 December 2025

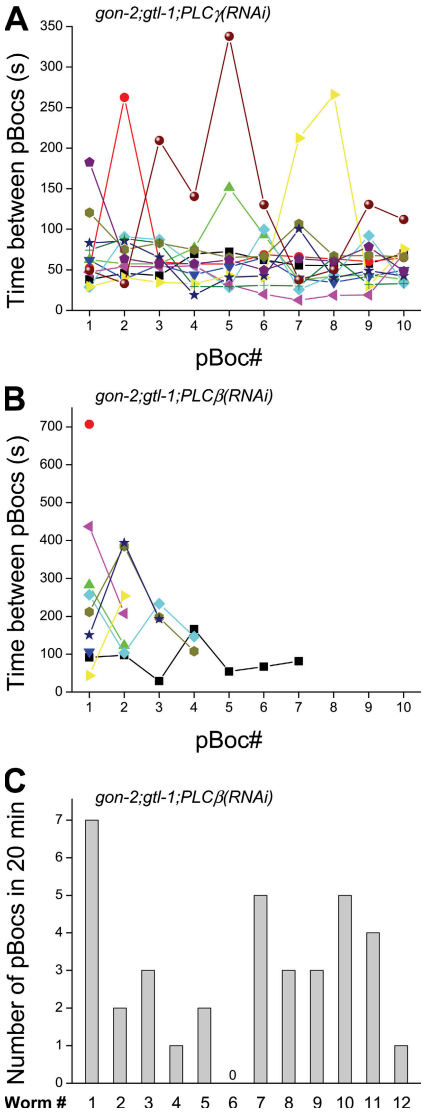

Figure 8. Effects of loss of PLCγ and PLCβ function on pBoc rhythmicity in *gon-2;gtl-1* double mutant worms. (A and B) pBoc cycles in individual *gon-2;gtl-1* mutant worms fed bacteria producing dsRNA homologous to either PLCγ (A) or PLCβ (B). Different colors and symbols represent different animals. (C) Number of pBocs measured in 12 *gon-2;gtl-1;PLCβ(RNAi)* worms over 20-min observation period.

Given the lack of effect we observed of high external Mg^{2+} concentration on pBoc and the high relative Ca^{2+} permeabilities of the ORCa, GON-2, and GTL-1 channels (Fig. 6 B), it is reasonable to postulate that they play a direct role in regulating and/or maintaining IP_3-dependent intestinal Ca^{2+} oscillations. To address this possibility, we performed genetic epistasis experiments. PLCγ and PLCβ homologues function together to regulate pBoc and generate Ca^{2+} oscillations in the *C. elegans* intestine. Loss of function of either enzyme causes striking arrhythmia of both pBoc and oscillatory Ca^{2+} signaling. Combined loss of function of both enzymes is additive giving rise to severe Ca^{2+} signaling and pBoc defects (Espelt et al., 2005). These results suggest that PLCγ and PLCβ function in different signaling pathways. Epistasis analysis using mutant alleles predicted to elevate intracellular IP_3 levels indicates that PLCγ functions primarily to generate IP_3 and regulate IP_3 receptor activity whereas PLCβ functions in a distinct and yet to be defined signaling pathway required for normal Ca^{2+} signaling (Espelt et al., 2005). The localization of PLCβ to sites of cell–cell contact (Miller et al., 1999) suggests that the enzyme may play a role in regulating intestinal Ca^{2+} waves that coordinate muscle contractions required for defecation (Peters et al., 2007).

To determine whether GON-2 and GTL-1 may play a role in the IP_3 receptor signaling pathway, we fed *gon-2;gtl-1* double mutant worms bacteria expressing dsRNA homologous to either PLCγ or PLCβ. As shown in Fig. 8 A, PLCγ RNAi had no additive effect on the pBoc arrhythmia induced by loss of function of both channels. Mean ± SEM pBoc period and coefficient of variance for *gon-2;gtl-1;PLCγ(RNAi)* worms were 73 ± 7 s and 49 ± 7% (n = 14). These values were not significantly ($P > 0.09$; see Fig. 2, A and B) different from that observed in *gon-2;gtl-1* double mutant worms fed normal bacteria. In contrast, knockdown of PLCβ in *gon-2;gtl-1* mutant worms induced a pBoc defect that was much more severe than that observed with the channel mutations alone (Fig. 8, B and C). Over a 20-min measurement period, no more than seven pBocs were observed in any of the *gon-2;gtl-1;plcβ(RNAi)* worms. The mean number of pBocs observed in 20 min in these animals was three (n = 12). One of the 12 animals examined exhibited no pBocs in this time period. This phenotype is remarkably similar to that induced by combined loss of function of PLCγ and PLCβ (Espelt et al., 2005) and suggests that GON-2 and GTL-1 function together with PLCγ to regulate IP_3 receptor activity and ER Ca^{2+} release.

DISCUSSION

The ORCa Channel Is Encoded by the TRPM Homologues *gon-2* and *gtl-1*

The TRP cation channel superfamily is subdivided into TRPC, TRPV, TRPM, TRPML, TRPP, TRPN, and TRPA subfamilies. All TRP channels are comprised of six predicted transmembrane domains and intracellular N and C termini. Functional TRP channels are formed from homomeric or heteromeric association of four TRP subunits. TRP channels function in diverse physiological processes including sensory transduction, epithelial transport of Ca^{2+} and Mg^{2+}, Ca^{2+} signaling, and modulation of membrane potential (Owsianik et al., 2006; Nilius et al., 2007).

The mammalian TRPM subfamily consists of TRPM1–8 (Kraft and Harteneck, 2005). GON-2 and GTL-1 share ~23% identity with TRPM1, TRPM3, TRPM6, and TRPM7 (Baylis and Goyal, 2007). The conserved structural motifs

Downloaded from http://rupress.org/jgp/article-pdf/131/3/245/1912627/jgp_200709914.pdf by guest on 05 December 2025

in these channels are the transmembrane domains, the TRP domain, and portions of the cytoplasmic N terminus.

Amino acids that comprise the pores of TRPM6 and TRPM7 have been identified by mutagenesis and patch clamp analysis (Chubanov et al., 2007; Li et al., 2007; Topala et al., 2007). The homologous pore domains are nearly identical in GON-2 and GTL-1. This is consistent with our findings that the two channels have similar biophysical properties (Figs. 5 and 6).

As shown in Fig. 4 A and Fig. 5 A, I_{ORCa} is dramatically inhibited by loss-of-function mutations in either *gon-2* or *gtl-1*. Loss of function of both genes completely eliminates the current (Fig. 4 B). There are two possible explanations for these results. Either the ORCa whole cell current is comprised of independent GON-2 and GTL-1 currents, or the ORCa channel is a GON-2/GTL-1 heteromer. Our results suggest that the function of GON-2 and GTL-1 are interdependent. The combined inhibition of I_{ORCa} observed in *gon-2* and *gtl-1* mutant cells is ~160% (Fig. 4 A). This finding indicates that GON-2 and GTL-1 can function independently as ion channels, but that maximal I_{ORCa} activity requires a functional interaction between them. One possibility is that the ORCa channel is a GON-2/GTL-1 heteromer. Alternatively, loss of either GON-2 or GTL-1 alone may disrupt the trafficking, expression, and/or regulation of the other channel.

Numerous studies have provided evidence that closely related TRP channels heteromultimerize (Owsianik et al., 2006; Nilius et al., 2007). Heteromultimers of TRPM6 and TRPM7, homologues of GON-2 and GTL-1, have been described (Chubanov et al., 2004; Li et al., 2006). At present, we favor the hypothesis that the ORCa channel is formed by association of GON-2 and GTL-1 subunits. However, extensive additional work including heterologous expression, mutagenesis, and subcellular localization of the two channels in vivo is required to test this idea.

Our electrophysiological findings differ from those of Teramoto et al. (2005). These investigators saw no effect of the *gtl-1* deletion allele on whole cell current, whereas the *gon-2* mutation reduced La^{3+}-inhibitable outward current at +100 mV ~75%. Current reduction was similar in intestinal cells cultured from *gon-2* and the *gon-2;gtl-1* double mutant worms. They also observed that the IC_{50} value for inhibition of the wild-type current by intracellular Mg^{2+} was 4.7-fold higher than that of the current observed in *gtl-1* mutant cells. In contrast, we found that I_{ORCa}, $I_{GON\text{-}2}$, and $I_{GTL\text{-}1}$ exhibit similar sensitivities to intracellular Mg^{2+} (Fig. 6 C). Teramoto et al. (2005) concluded that GON-2 mainly mediates the outwardly rectifying current and that GTL-1 functions mainly to regulate current Mg^{2+} responsiveness. The reasons for the differences in our findings are unclear.

Role of GON-2 and GTL-1 in Oscillatory Ca^{2+} Signaling

Most TRP channels described to date have no or relatively low selectivity for Ca^{2+} over Na^+ (Owsianik et al., 2006). The exceptions to this generalization are TRPV5 and TRPV6, which have P_{Ca}/P_{Na} values >100 and play important roles in epithelial Ca^{2+} absorption (Vennekens et al., 2000; Yue et al., 2001; Owsianik et al., 2006). GON-2, GTL-1, and the ORCa channels exhibit a >60-fold selectivity for Ca^{2+} over Na^+ (Fig. 6 B; Estevez et al., 2003). Mammalian TRPM channels are either impermeable to Ca^{2+} (TRPM4 and TRPM5) or have P_{Ca}/P_{Na} values of 0.1–10 (Owsianik et al., 2006). Heterologously expressed *Drosophila* TRP and TRPL have relative Ca^{2+} permeabilities of 10–12 (Xu et al., 1997). Studies of the native TRP current in wild-type *Drosophila* photoreceptor cells indicate that the channel(s) responsible for the current are ~40-fold more permeable to Ca^{2+} than monovalent cations (Hardie and Minke, 1992; Reuss et al., 1997). The endogenous Ca^{2+} conductances in *trp* and *trpl* mutant photoreceptor cells have P_{Ca}/P_{Na} values of ~4 and ~86, respectively (Hardie and Minke, 1992; Reuss et al., 1997). Thus, together with mammalian TRPV5/6 and possibly *Drosophila* TRP, GON-2, GTL-1, and the ORCa channels have the highest Ca^{2+} selectivity of all characterized TRPs.

Given their exceptionally high Ca^{2+} selectivity and essential roles in maintaining pBoc and Ca^{2+} signaling rhythmicity (Fig. 2 and 3), what possible functions could GON-2 and GTL-1 be performing? Data in Fig. 8 suggest that the channels function in a signaling pathway together with PLCγ to regulate IP_3 receptor activity. Our previous studies failed to identify a significant role for the canonical store-operated CRAC channel in maintaining intestinal Ca^{2+} oscillations (Lorin-Nebel et al., 2007; Yan et al., 2006). Thus other Ca^{2+} channels must provide a Ca^{2+} entry pathway that allows for store refilling. It is conceivable that GON-2 and GTL-1 function in part to refill ER Ca^{2+} stores. However, even in the absence of these channels Ca^{2+} oscillations continue albeit arrhythmically (Figs. 2 and 3). This indicates that other Ca^{2+} entry pathways must function in the intestine to refill stores under these experimental conditions.

An attractive possibility is that the GON-2 and GTL-1 channels play a direct role in modulating IP_3 receptor activity and controlling oscillation frequency. It is well established that IP_3 receptors are regulated in a biphasic manner by intracellular Ca^{2+}; low levels of Ca^{2+} activate the channels whereas high Ca^{2+} levels feedback and inhibit channel activity (Foskett et al., 2007). Foskett and coworkers (Mak et al., 1998; Foskett et al., 2007) have argued that Ca^{2+} is a true IP_3 receptor agonist and that IP_3 functions only to relieve Ca^{2+} inhibition. In excitable cells, plasma membrane Ca^{2+} influx through voltage- and ligand-gated Ca^{2+} channels can trigger intracellular Ca^{2+} release through ryanodine receptors via a process termed Ca^{2+}-induced Ca^{2+} release (CICR) (Berridge et al., 2003). Plasma membrane Ca^{2+} influx can also trigger CICR via IP_3 receptors (e.g., Kukuljan et al., 1997; Kapur et al., 2001; Gordienko et al., 2007).

Downloaded from http://rupress.org/jgp/article-pdf/131/3/245/1912627/jgp_200709914.pdf by guest on 05 December 2025

The disruption of Ca^{2+} oscillation rhythmicity in *gon-2* and *gtl-1* mutants (Figs. 2 and 3) suggests that the channels function as part of the timekeeping apparatus that regulates cycle periodicity. We have shown previously that under conditions of low intracellular Ca^{2+} buffering, ORCa channel activity oscillates. Oscillating channel activity is due to a Ca^{2+} feedback mechanism similar to that observed with the IP_3 receptor (Estevez and Strange, 2005). Such oscillating channel activity could provide a source of extracellular Ca^{2+} that functions to modulate IP_3 receptor activity. Specifically, Ca^{2+} influx through ORCa channels could trigger IP_3 receptor–mediated Ca^{2+} release via CICR. Rising cytoplasmic Ca^{2+} levels would feedback on both the IP_3 receptor and ORCa channels functioning initially to increase and than eventually inhibit their activity. Calcium influx through ORCa channels would raise Ca^{2+} levels in channel microdomains and may also contribute to the overall increase in cytoplasmic Ca^{2+}. Microdomain Ca^{2+} increases as well as the amplitude of the cytoplasmic Ca^{2+} increase would likely play a role in triggering downstream cellular functions.

Several TRP channels are known to be regulated by intracellular Ca^{2+} and play important roles in Ca^{2+} signaling. For example, the nonselective cation channel TRPM4 is activated by increases in intracellular Ca^{2+} (Launay et al., 2002). In T cells, TRPM4-mediated membrane depolarization modulates Ca^{2+} influx via CRAC channels and controls oscillatory Ca^{2+} signaling (Launay et al., 2004). TRPM5 is activated by intracellular Ca^{2+} concentrations of 0.3–1 μM and inhibited by higher Ca^{2+} levels and may function to couple intracellular Ca^{2+} release to membrane electrical activity (Prawitt et al., 2003). TRPC3 shows modest Ca^{2+} selectivity and initiates Ca^{2+} oscillations when activated by OAG. Increasing intracellular Ca^{2+} levels inhibits the channel (Grimaldi et al., 2003). Extensive additional studies using Ca^{2+} imaging, patch clamp electrophysiology, molecular biology, and forward and reverse genetics are needed to define the precise roles played by GON-2 and GTL-1 in intestinal Ca^{2+} signaling.

In conclusion, we have demonstrated that I_{ORCa} requires the combined function of the TRPM genes *gon-2* and *gtl-1*. GON-2 and GTL-1 are highly Ca^{2+}-selective channels and are essential for maintaining rhythmic Ca^{2+} oscillations in the *C. elegans* intestine. We postulate that GON-2 and GTL-1 form a heteromeric channel that selectively mediates Ca^{2+} influx and functions primarily to regulate IP_3 receptor activity and possibly to refill ER Ca^{2+} stores.

We thank Dr. Jerod Denton for critically reviewing the manuscript and for many helpful discussions, Dr. Joel Rothman for providing the *elt-2*::GFP-expressing worm strain, and Dr. Eric Lambie for providing the *gon-2(q388)* and *gon-2;gtl-1* double mutant worm strains. Other strains used in this work were provided by the *Caenorhabditis* Genetics Center (University of Minnesota, Minneapolis, MN).

This work was supported by National Institutes of Health grant GM74229 to K. Strange.

Lawrence G. Palmer served as editor.

Submitted: 24 October 2007
Accepted: 30 January 2008

REFERENCES

Barr, M.M. 2003. Super models. *Physiol. Genomics.* 13:15–24.

Baylis, H.A., and K. Goyal. 2007. TRPM channel function in *Caenorhabditis elegans*. *Biochem. Soc. Trans.* 35:129–132.

Berridge, M.J., M.D. Bootman, and H.L. Roderick. 2003. Calcium signalling: dynamics, homeostasis and remodelling. *Nat. Rev. Mol. Cell Biol.* 4:517–529.

Brenner, S. 1974. The genetics of *Caenorhabditis elegans*. *Genetics.* 77:71–94.

Christensen, M., A.Y. Estevez, X.M. Yin, R. Fox, R. Morrison, M. McDonnell, C. Gleason, D.M. Miller, and K. Strange. 2002. A primary culture system for functional analysis of *C. elegans* neurons and muscle cells. *Neuron.* 33:503–514.

Chubanov, V., K.P. Schlingmann, J. Waring, J. Heinzinger, S. Kaske, S. Waldegger, M.M. Schnitzler, and T. Gudermann. 2007. Hypomagnesemia with secondary hypocalcemia due to a missense mutation in the putative pore-forming region of TRPM6. *J. Biol. Chem.* 282:7656–7667.

Chubanov, V., S. Waldegger, M. Schnitzler, H. Vitzthum, M.C. Sassen, H.W. Seyberth, M. Konrad, and T. Gudermann. 2004. Disruption of TRPM6/TRPM7 complex formation by a mutation in the TRPM6 gene causes hypomagnesemia with secondary hypocalcemia. *Proc. Natl. Acad. Sci. USA.* 101:2894–2899.

Church, D.L., and E.J. Lambie. 2003. The promotion of gonadal cell divisions by the *Caenorhabditis elegans* TRPM cation channel GON-2 is antagonized by GEM-4 copine. *Genetics.* 165:563–574.

Dal Santo, P., M.A. Logan, A.D. Chisholm, and E.M. Jorgensen. 1999. The inositol trisphosphate receptor regulates a 50-second behavioral rhythm in *C. elegans*. *Cell.* 98:757–767.

Espelt, M.V., A.Y. Estevez, X. Yin, and K. Strange. 2005. Oscillatory Ca^{2+} signaling in the isolated *Caenorhabditis elegans* intestine: role of the inositol-1,4,5-trisphosphate receptor and phospholipases C β and γ. *J. Gen. Physiol.* 126:379–392.

Estevez, A.Y., R.K. Roberts, and K. Strange. 2003. Identification of store-independent and store-operated Ca^{2+} conductances in *Caenorhabditis elegans* intestinal epithelial cells. *J. Gen. Physiol.* 122:207–223.

Estevez, A.Y., and K. Strange. 2005. Calcium feedback mechanisms regulate oscillatory activity of a TRP-like Ca^{2+} conductance in *C. elegans* intestinal cells. *J. Physiol.* 567:239–251.

Foskett, J.K., C. White, K.H. Cheung, and D.O. Mak. 2007. Inositol trisphosphate receptor Ca^{2+} release channels. *Physiol. Rev.* 87:593–658.

Fukushige, T., M.G. Hawkins, and J.D. McGhee. 1998. The GATA-factor *elt-2* is essential for formation of the *Caenorhabditis elegans* intestine. *Dev. Biol.* 198:286–302.

Gordienko, D.V., M.I. Harhun, M.V. Kustov, V. Pucovsky, and T.B. Bolton. 2007. Sub-plasmalemmal $[Ca^{2+}]_i$ upstroke in myocytes of the guinea-pig small intestine evoked by muscarinic stimulation: IP3R-mediated Ca^{2+} release induced by voltage-gated Ca^{2+} entry. *Cell Calcium.* 43:122–141.

Grimaldi, M., M. Maratos, and A. Verma. 2003. Transient receptor potential channel activation causes a novel form of $[Ca^{2+}]_i$ oscillations and is not involved in capacitative Ca^{2+} entry in glial cells. *J. Neurosci.* 23:4737–4745.

Hardie, R.C., and B. Minke. 1992. The trp gene is essential for a light-activated Ca^{2+} channel in *Drosophila* photoreceptors. *Neuron.* 8:643–651.

Hogan, P.G., and A. Rao. 2007. Dissecting I_{CRAC}, a store-operated calcium current. *Trends Biochem. Sci.* 32:235–245.

Iwasaki, K., D.W. Liu, and J.H. Thomas. 1995. Genes that control a temperature-compensated ultradian clock in *Caenorhabditis elegans*. *Proc. Natl. Acad. Sci. USA.* 92:10317–10321.

Downloaded from http://rupress.org/jgp/article-pdf/131/3/245/1912627/jgp_200709914.pdf by guest on 05 December 2025

Kahn-Kirby, A.H., and C.I. Bargmann. 2006. TRP channels in *C. elegans*. *Annu. Rev. Physiol.* 68:719–736.

Kamath, R.S., M. Martinez-Campos, P. Zipperlen, A.G. Fraser, and J. Ahringer. 2000. Effectiveness of specific RNA-mediated interference through ingested double-stranded RNA in *Caenorhabditis elegans*. *Genome Biol.* 2:research0002.1-0002.10. doi:10.1186/gb-2000-2-1-research0002.

Kapur, A., M. Yeckel, and D. Johnston. 2001. Hippocampal mossy fiber activity evokes Ca^{2+} release in CA3 pyramidal neurons via a metabotropic glutamate receptor pathway. *Neuroscience.* 107:59–69.

Kraft, R., and C. Harteneck. 2005. The mammalian melastatin-related transient receptor potential cation channels: an overview. *Pflugers Arch.* 451:204–211.

Kukuljan, M., L. Vergara, and S.S. Stojilkovic. 1997. Modulation of the kinetics of inositol 1,4,5-trisphosphate-induced $[Ca^{2+}]_i$ oscillations by calcium entry in pituitary gonadotrophs. *Biophys. J.* 72:698–707.

Launay, P., H. Cheng, S. Srivatsan, R. Penner, A. Fleig, and J.P. Kinet. 2004. TRPM4 regulates calcium oscillations after T cell activation. *Science.* 306:1374–1377.

Launay, P., A. Fleig, A.L. Perraud, A.M. Scharenberg, R. Penner, and J.P. Kinet. 2002. TRPM4 is a Ca^{2+}-activated nonselective cation channel mediating cell membrane depolarization. *Cell.* 109:397–407.

Lewis, R.S. 2007. The molecular choreography of a store-operated calcium channel. *Nature.* 446:284–287.

Li, M., J. Du, J. Jiang, W. Ratzan, L.T. Su, L.W. Runnels, and L. Yue. 2007. Molecular determinants of Mg^{2+} and Ca^{2+} permeability and pH sensitivity in TRPM6 and TRPM7. *J. Biol. Chem.* 282:25817–25830.

Li, M., J. Jiang, and L. Yue. 2006. Functional characterization of homo- and heteromeric channel kinases TRPM6 and TRPM7. *J. Gen. Physiol.* 127:525–537.

Liu, D.W., and J.H. Thomas. 1994. Regulation of a periodic motor program in *C. elegans*. *J. Neurosci.* 14:1953–1962.

Lorin-Nebel, C., J. Xing, X. Yan, and K. Strange. 2007. CRAC channel activity in *C. elegans* is mediated by Orai1 and STIM1 homologs and is essential for ovulation and fertility. *J. Physiol.* 580:67–85.

Mak, D.O., S. McBride, and J.K. Foskett. 1998. Inositol 1,4,5-trisphosphate activation of inositol trisphosphate receptor Ca^{2+} channel by ligand tuning of Ca^{2+} inhibition. *Proc. Natl. Acad. Sci. USA.* 95:15821–15825.

Miller, K.G., M.D. Emerson, and J.B. Rand. 1999. Goα and diacylglycerol kinase negatively regulate the Gqα pathway in *C. elegans*. *Neuron.* 24:323–333.

Nilius, B., G. Owsianik, T. Voets, and J.A. Peters. 2007. Transient receptor potential cation channels in disease. *Physiol. Rev.* 87:165–217.

Owsianik, G., K. Talavera, T. Voets, and B. Nilius. 2006. Permeation and selectivity of TRP channels. *Annu. Rev. Physiol.* 68:685–717.

Parekh, A.B., and J.W. Putney. 2005. Store-operated calcium channels. *Physiol. Rev.* 85:757–810.

Peters, M.A., T. Teramoto, J.Q. White, K. Iwasaki, and E.M. Jorgensen. 2007. A calcium wave mediated by gap junctions coordinates a rhythmic behavior in *C. elegans*. *Curr. Biol.* 17:1601–1608.

Prawitt, D., M.K. Monteilh-Zoller, L. Brixel, C. Spangenberg, B. Zabel, A. Fleig, and R. Penner. 2003. TRPM5 is a transient Ca^{2+}-activated cation channel responding to rapid changes in $[Ca^{2+}]_i$. *Proc. Natl. Acad. Sci. USA.* 100:15166–15171.

Putney, J.W. Jr. 2007. Recent breakthroughs in the molecular mechanism of capacitative calcium entry (with thoughts on how we got here). *Cell Calcium.* 42:103–110.

Reuss, H., M.H. Mojet, S. Chyb, and R.C. Hardie. 1997. In vivo analysis of the *Drosophila* light-sensitive channels, TRP and TRPL. *Neuron.* 19:1249–1259.

Rual, J.F., J. Ceron, J. Koreth, T. Hao, A.S. Nicot, T. Hirozane-Kishikawa, J. Vandenhaute, S.H. Orkin, D.E. Hill, H.S. van den, and M. Vidal. 2004. Toward improving *Caenorhabditis elegans* phenome mapping with an ORFeome-based RNAi library. *Genome Res.* 14:2162–2168.

Strange, K. 2003. From genes to integrative physiology: ion channel and transporter biology in *Caenorhabditis elegans*. *Physiol. Rev.* 83:377–415.

Strange, K., M. Christensen, and R. Morrison. 2007. Primary culture of *Caenorhabditis elegans* developing embryo cells for electrophysiological, cell biological and molecular studies. *Nat. Protoc.* 2:1003–1012.

Sun, A.Y., and E.J. Lambie. 1997. *gon-2*, a gene required for gonadogenesis in *Caenorhabditis elegans*. *Genetics.* 147:1077–1089.

Teramoto, T., and K. Iwasaki. 2006. Intestinal calcium waves coordinate a behavioral motor program in *C. elegans*. *Cell Calcium.* 40:319–327.

Teramoto, T., E.J. Lambie, and K. Iwasaki. 2005. Differential regulation of TRPM channels governs electrolyte homeostasis in the *C. elegans* intestine. *Cell Metab.* 1:343–354.

Thomas, J.H. 1990. Genetic analysis of defecation in *Caenorhabditis elegans*. *Genetics.* 124:855–872.

Topala, C.N., W.T. Groenestege, S. Thebault, B.D. van den, B. Nilius, J.G. Hoenderop, and R.J. Bindels. 2007. Molecular determinants of permeation through the cation channel TRPM6. *Cell Calcium.* 41:513–523.

Venkatachalam, K., D.B. van Rossum, R.L. Patterson, H.T. Ma, and D.L. Gill. 2002. The cellular and molecular basis of store-operated calcium entry. *Nat. Cell Biol.* 4:E263–E272.

Vennekens, R., J.G. Hoenderop, J. Prenen, M. Stuiver, P.H. Willems, G. Droogmans, B. Nilius, and R.J. Bindels. 2000. Permeation and gating properties of the novel epithelial Ca^{2+} channel. *J. Biol. Chem.* 275:3963–3969.

West, R.J., A.Y. Sun, D.L. Church, and E.J. Lambie. 2001. The *C. elegans gon-2* gene encodes a putative TRP cation channel protein required for mitotic cell cycle progression. *Gene.* 266:103–110.

Xu, X.Z., H.S. Li, W.B. Guggino, and C. Montell. 1997. Coassembly of TRP and TRPL produces a distinct store-operated conductance. *Cell.* 89:1155–1164.

Yan, X., J. Xing, C. Lorin-Nebel, A.Y. Estevez, K. Nehrke, T. Lamitina, and K. Strange. 2006. Function of a STIM1 homologue in *C. elegans*: evidence that store-operated Ca^{2+} entry is not essential for oscillatory Ca^{2+} signaling and ER Ca^{2+} homeostasis. *J. Gen. Physiol.* 128:443–459.

Yeromin, A.V., J. Roos, K.A. Stauderman, and M.D. Cahalan. 2004. A store-operated calcium channel in *Drosophila* S2 cells. *J. Gen. Physiol.* 123:167–182.

Yin, X., N.J. Gower, H.A. Baylis, and K. Strange. 2004. Inositol 1,4,5-trisphosphate signaling regulates rhythmic contractile activity of smooth muscle-like sheath cells in the nematode *Caenorhabditis elegans*. *Mol. Biol. Cell.* 15:3938–3949.

Yue, L., J.B. Peng, M.A. Hediger, and D.E. Clapham. 2001. CaT1 manifests the pore properties of the calcium-release-activated calcium channel. *Nature.* 410:705–709.

Downloaded from http://rupress.org/jgp/article-pdf/131/3/245/1912627/jgp_200709914.pdf by guest on 05 December 2025